Magnetic properties of disordered Ising ternary alloys

1998 J. Phys.: Condens. Matter 10 5359

(http://iopscience.iop.org/0953-8984/10/24/013)

J. Phys.: Condens. Matter **10** (1998) 5359–5372. Printed in the UK PII: S0953-8984(98)90229-6

Magnetic properties of disordered Ising ternary alloys

T Kaneyoshi and Y Nakamura

Department of Natural Science Informatics, School of Informatics and Sciences, Nagoya University, 464-01, Nagoya, Japan

Received 29 December 1997, in final form 10 February 1998

Abstract. A theoretical framework for treating a disordered Ising ternary alloy $(A_pB_{1-p})_rC_{1-r}$ where A and B represent magnetic atoms and C represents non-magnetic atoms is discussed within the effective-field theory with correlations. The magnetic properties of some disordered alloys with spins $S_A = \frac{1}{2}$ and $S_B = \frac{1}{2}$ (or $S_B = \frac{3}{2}$) are investigated within the framework. We find some characteristic phenomena for a ferrimagnetic alloy with $S_B = \frac{3}{2}$, such as an interesting effect of non-magnetic atoms on a compensation point (or points).

1. Introduction

The magnetic properties of a disordered Ising binary alloy A_pB_{1-p} in which the lattice sites are randomly occupied by two different types of magnetic atom (A and B, with spins S_A and S_B) have been investigated by many authors, using a variety of theoretical methods (molecular-field theory, effective-field theory, CPA, Monte Carlo simulation). In these studies, there has been some interest shown in the phase diagrams of a disordered binary alloy consisting of spins $S_A = S_B = \frac{1}{2}$, with a transition temperature $T_C(p)$ as a function of concentration p [1–3]. The phase diagrams have been usefully classified in terms of the initial slopes $\partial \ln T_C(p)/\partial p$ of T_C at $p = 1$ and $p = 0$, and six (or seven) phases have been obtained from the possible nine phases, while molecular-field theory (MFT) predicts only four possible phases. On the other hand, some attention has been paid to the study of ferrimagnetic disordered binary alloys. In particular, Kaneyoshi *et al* [4–6] have proposed recently the possibility of many compensation points in a disordered Ising ferrimagnetic binary alloy with $S_A = \frac{1}{2}$ and $S_B > \frac{1}{2}$ as well as a thin ferrimagnetic film.

Amorphous ferromagnetic (or ferrimagnetic) alloys, in particular transition metal–metalloid (or rare-earth–transition metal–metalloid) glasses, have been well studied experimentally for the purpose of fundamental research and with a view to technological applications [7, 8]. They can be described by the general formula $(A_pB_{1-p})_rC_{1-r}$ where A and B represent magnetic atoms with concentrations pr and $(1-p)r$, respectively, and C is the non-magnetic metalloid with concentration $1-r$. The concentration dependence of T_C has been intensively investigated experimentally, and a good correspondence between experimental data and mean-field-type predictions can be found in [9]. The temperature dependence of the total magnetization has been analysed by the use of the MFT [7]. As far as we are aware, however, the magnetic properties of a disordered ferrimagnetic Ising ternary alloy have not been discussed so far theoretically using a sophisticated theory superior to the MFT. In particular, the effects of non-magnetic atoms on a compensation point (or points) in the ferrimagnetic alloy have not been discussed.

0953-8984/98/245359+14$19.50

The aim of this work is to study the theoretical framework for a disordered Ising ternary alloy $(A_pB_{1-p})_rC_{1-r}$ with $S_A = \frac{1}{2}$ and $S_B = S$ ($\geqslant \frac{1}{2}$) in the effective-field theory with correlations (EFT) [10, 11], which is superior to the MFT. The formulation is discussed in section 2. In section 3, the initial slopes $\partial \ln T_C(p)/\partial p$ at $p = 1$ and $p = 0$ for a disordered Ising ternary alloy with $S_A = S_B = \frac{1}{2}$ are investigated, and the phase diagrams are examined numerically for the system with the coordination number $z = 4$. In section 4, we study the magnetic properties of a disordered Ising ferrimagnetic ternary alloy with $S_A = \frac{1}{2}$ and $S_B = \frac{3}{2}$. The effects of non-magnetic atoms on these properties are clarified numerically in sections 3 and 4.

2. Formulation

We consider a ternary Ising alloy of the type $(A_pB_{1-p})_rC_{1-r}$ with sites randomly occupied by three different species, where A and B are magnetic atoms and the C atoms are non-magnetic. The Hamiltonian of the system is given by

$$H = -\sum_{(ij)} \sum_{\nu,\nu'=\mathrm{A\,or\,B}} J_{\nu\nu'} S_{i\nu}^z S_{j\nu'}^z n_{i\nu} n_{j\nu'} \xi_i \xi_j - D \sum_i (S_{iB}^z)^2 n_{iB} \xi_i \tag{1}$$

where the $J_{\nu\nu'}$ are the exchange interactions between type-ν and type-ν' atoms (or $J_{AA} = J_A$, $J_{AB} = J_{BA}$, $J_{BB} = J_B$), the $S_{i\nu}^z$ are the spin variables of the type-ν atoms, $n_{i\nu} = 1$ if the spin i is of type ν, and 0 otherwise, and the $\sum_{(ij)}$ refers to all nearest neighbours. ξ_i is a random variable whose averaged value is given by $\langle \xi_i \rangle_r = r$ when the site i is occupied by a magnetic atom. The averaged value of $n_{i\nu}$ is then given by $\langle n_{i\nu} \rangle_r = p$ when $\nu = A$ and $\langle n_{i\nu} \rangle_r = 1 - p$ when $\nu = B$. D is the crystal-field interaction constant of a B atom, appearing when $S_B > \frac{1}{2}$. The total magnetization M of the system is given by

$$\frac{M}{N} = r[pm_A + (1-p)m_B] \tag{2}$$

where N is the total number of atoms, and the averaged magnetizations are defined by

$$m_A = \frac{\langle n_{iA} \xi_i \langle S_{iA}^z \rangle \rangle_r}{\langle n_{iA} \xi_i \rangle_r} \qquad m_B = \frac{\langle n_{iB} \xi_i \langle S_{iB}^z \rangle \rangle_r}{\langle n_{iB} \xi_i \rangle_r} \tag{3}$$

with

$$\langle n_{iA} \xi_i \rangle_r = rp$$

and

$$\langle n_{iB} \xi_i \rangle_r = r(1-p).$$

Using both the Ising spin identity and the differential operator technique ([10, 11], and see the review [12]), the averaged magnetizations can be exactly represented in the forms

$$m_A = \frac{1}{\langle n_{iA} \xi_i \rangle_r} \left\langle n_{iA} \xi_i \left\langle \prod_j \left[1 - \xi_j + n_{jA} \xi_j \left\{ \cosh\left(\frac{J_A}{2} \nabla \right) + 2 S_{jA}^z \sinh\left(\frac{J_A}{2} \nabla \right) \right\} \right.\right.\right.$$
$$\left.\left.\left. + n_{jB} \xi_j \left\{ \cosh(J_{AB} \eta \nabla) + \frac{S_{jB}^z}{\eta} \sinh(J_{AB} \eta \nabla) \right\} \right] \right\rangle\right\rangle_r F_A(x) \Big|_{x=0} \tag{4a}$$

$$m_B = \frac{1}{\langle n_{iB} \xi_i \rangle_r} \left\langle n_{iA} \xi_i \left\langle \prod_j \left[1 - \xi_j + n_{jA} \xi_j \left\{ \cosh\left(\frac{J_{AB}}{2} \nabla \right) + 2 S_{jA}^z \sinh\left(\frac{J_{AB}}{2} \nabla \right) \right\} \right.\right.\right.$$
$$\left.\left.\left. + n_{jB} \xi_j \left\{ \cosh(J_A \eta \nabla) + \frac{S_{jB}^z}{\eta} \sinh(J_B \eta \nabla) \right\} \right] \right\rangle\right\rangle_r F_B(x) \Big|_{x=0} \tag{4b}$$

where $\nabla = \partial/\partial x$ is a differential operator. The parameter η defined when $S_B > \frac{1}{2}$ is given by

$$\eta^2 = \frac{\langle n_{iB}\xi_i \langle (S_{iB}^z)^2 \rangle \rangle_r}{\langle n_{iB}\xi_i \rangle_r} = \frac{1}{\langle n_{iB}\xi_i \rangle_r} \left\langle n_{iB}\xi_i \left\langle \prod_j \left[1 - \xi_j + n_{jA}\xi_j \left\{ \cosh\left(\frac{J_{AB}}{2}\nabla \right) + 2S_{jA}^z \sinh\left(\frac{J_{AB}}{2}\nabla \right) \right\} + n_{jB}\xi_j \left\{ \cosh(J_B\eta\nabla) + \frac{S_{jB}^z}{\eta} \sinh(J_B\eta\nabla) \right\} \right] \right\rangle \right\rangle_r G_B(x)\Big|_{x=0}. \tag{5}$$

The function $F_A(x)$ is

$$F_A(x) = \frac{1}{2}\tanh\left(\frac{\beta x}{2} \right) \tag{6}$$

and the functions $F_B(x)$ and $G_B(x)$ are dependent on the value of S_B, and are given by

$$\begin{aligned} F_B(x) &= \frac{3\sinh(3\beta x/2) + \exp(-2D\beta)\sinh(\beta x/2)}{2\cosh(3\beta x/2) + 2\exp(-2D\beta)\cosh(\beta x/2)} \\ G_B(x) &= \frac{9\cosh(3\beta x/2) + \exp(-2D\beta)\cosh(\beta x/2)}{2\cosh(3\beta x/2) + 2\exp(-2D\beta)\cosh(\beta x/2)} \end{aligned} \tag{7}$$

for $S_B = \frac{3}{2}$, where $\beta = 1/k_B T$.

Here, it is clear that, if we try to treat all of the spin–spin correlations appearing through the expansions of (4) exactly, the problem becomes mathematically intractable. In the EFT, the decoupling approximation, or

$$\langle \langle x_{iv} x_{jv'} \cdots x_{kv''} \rangle \rangle_r \approx \langle \langle x_{iv} \rangle \rangle_r \langle \langle x_{jv'} \rangle \rangle_r \cdots \langle \langle x_{kv''} \rangle \rangle_r \tag{8}$$

with $i \neq j \neq \cdots \neq k$ and $x_{iv} = S_{iv}^z n_{iv}\xi_i$, has been used. In fact, this approximation corresponds to the Zernike approximation for the spin-$\frac{1}{2}$ Ising ferromagnet [12]. The approximation has been successfully applied to a great number of magnetic systems. Within the EFT, the magnetizations (4) and the equation (5) are given by

$$m_A = \left[1 - r + rp \left\{ \cosh\left(\frac{J_A}{2}\nabla \right) + 2m_A \sinh\left(\frac{J_A}{2}\nabla \right) \right\} + r(1-p) \left\{ \cosh(J_{AB}\eta\nabla) + \frac{m_B}{\eta} \sinh(J_{AB}\eta\nabla) \right\} \right]^z F_A(x)\Big|_{x=0} \tag{9a}$$

$$m_B = \left[1 - r + rp \left\{ \cosh\left(\frac{J_{AB}}{2}\nabla \right) + 2m_A \sinh\left(\frac{J_{AB}}{2}\nabla \right) \right\} + r(1-p) \left\{ \cosh(J_B\eta\nabla) + \frac{m_B}{\eta} \sinh(J_B\eta\nabla) \right\} \right]^z F_B(x)\Big|_{x=0} \tag{9b}$$

and

$$\eta^2 = \left[1 - r + rp \left\{ \cosh\left(\frac{J_{AB}}{2}\nabla \right) + 2m_A \sinh\left(\frac{J_{AB}}{2}\nabla \right) \right\} + r(1-p) \left\{ \cosh(J_B\eta\nabla) + \frac{m_B}{\eta} \sinh(J_B\eta\nabla) \right\} \right]^z G_B(x)\Big|_{x=0} \tag{9c}$$

where z is the coordination number.

We are now interested in investigating the magnetic properties of a disordered Ising ternary alloy. The problems are examined in the following sections by selecting separately two values of S_B, namely $S_B = \frac{1}{2}$ and $S_B = \frac{3}{2}$.

3. Phase diagrams of a system with $S_B = 1/2$

In this section, let us study the phase diagram of a disordered Ising ternary alloy with $S_A = S_B = \frac{1}{2}$. With this aim, we use the usual argument that m_α ($\alpha = A$ or B) tends to zero as the temperature approaches a critical temperature, which allows us to consider just terms linear in m_α. In particular, the parameter η for the system with $S_B = \frac{1}{2}$ is exactly given by $\eta = \frac{1}{2}$ [11]. By the use of these procedures, the critical temperature T_C (or phase diagram) of a disordered ternary alloy can be determined by solving the relation

$$[2zrpK_1 - 1][2zr(1-p)K_4 - 1] = 4(zr)2p(1-p)K_2K_3 \tag{10}$$

with

$$K_1 = \sinh\left(\frac{J_A}{2}\nabla\right)\left[1 - r + rp\cosh\left(\frac{J_A}{2}\nabla\right) + r(1-p)\cosh\left(\frac{J_{AB}}{2}\nabla\right)\right]^{z-1} f(x)\Big|_{x=0} \tag{11a}$$

$$K_2 = \sinh\left(\frac{J_{AB}}{2}\nabla\right)\left[1 - r + rp\cosh\left(\frac{J_A}{2}\nabla\right) + r(1-p)\cosh\left(\frac{J_{AB}}{2}\nabla\right)\right]^{z-1} f(x)\Big|_{x=0} \tag{11b}$$

$$K_3 = \sinh\left(\frac{J_{AB}}{2}\nabla\right)\left[1 - r + rp\cosh\left(\frac{J_{AB}}{2}\nabla\right) + r(1-p)\cosh\left(\frac{J_B}{2}\nabla\right)\right]^{z-1} f(x)\Big|_{x=0} \tag{11c}$$

$$K_4 = \sinh\left(\frac{J_B}{2}\nabla\right)\left[1 - r + rp\cosh\left(\frac{J_{AB}}{2}\nabla\right) + r(1-p)\cosh\left(\frac{J_B}{2}\nabla\right)\right]^{z-1} f(x)\Big|_{x=0} \tag{11d}$$

where the function $f(x)$ is defined by $f(x) = F_B(x) = F_A(x)$ given by (6). T_C depends on the values of J_A, J_{AB}, J_B, p, r and z. In particular, one should be aware of the following facts.

(i) T_C determined from (10) is independent of the sign of J_{AB}, or (10) is valid for the ferromagnetic ($J_{AB} > 0$) case as well as for the antiferromagnetic ($J_{AB} < 0$) case.

(ii) When $r = 1$, the relation (10) is equivalent to that for a disordered binary alloy discussed in [2].

The initial slopes $\partial \ln T_C(p)/\partial p$ at $p = 1$ and $p = 0$ can be obtained by differentiating (10) with respect to p. Without loss of generality, we suppose that $T_C(p = 1) > T_C(p = 0)$ (or $J_A > J_B$) and also that $J_{AB} > 0$ for studying the phase diagram. Then, the simplest possible phase boundary is a straight-line extrapolation for $T_C(p)$ between $T_C(0)$ and $T_C(1)$. Furthermore, the three possible types of behaviour can be identified from the initial slopes at $p = 0$: (1) a slope greater than that of the linear extrapolation, (2) a slope less than that of the linear extrapolation but greater than zero, and (3) a slope less than zero. There are also three similar types of behaviour at $p = 1$. These phase boundaries can be given by the following relations:

$$\left[\frac{\partial \ln T_C(p)}{\partial p}\right]_{p=1} = 0 \tag{12a}$$

$$\left[\frac{\partial \ln T_C(p)}{\partial p}\right]_{p=1} = \frac{T_C(p=1) - T_C(p=0)}{T_C(p=1)} \tag{12b}$$

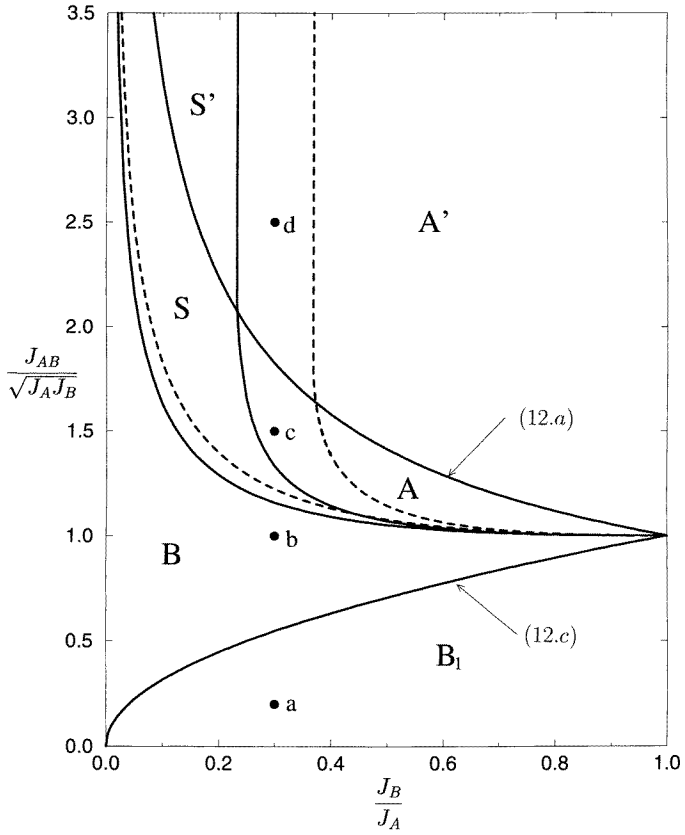

Figure 1. Possible kinds of phase diagram in the space $(J_{AB}/\sqrt{J_A J_B}, J_B/J_A)$ of the Ising ferromagnetic ternary alloy with $z = 4$ (on a square lattice), when the two values of r are selected. In particular, the results for $r = 1$ (solid lines) are equivalent to those for the Ising binary alloy [2]. The dashed lines represent the results for $r = 0.7$. The six kinds of phase diagram (S, S′, A, A′, B and B_1) are shown, where the nomenclature of [1] is used. The black points a–d are the points for which the complete phase boundaries are shown in figure 2.

$$\left[\frac{\partial \ln T_C(p)}{\partial p}\right]_{p=0} = 0 \tag{12c}$$

$$\left[\frac{\partial \ln T_C(p)}{\partial p}\right]_{p=0} = \frac{T_C(p=1) - T_C(p=0)}{T_C(p=0)}. \tag{12d}$$

Nine phase diagrams may be possible from these phase boundaries. But, one should note the following facts. The initial slopes by no means provide a complete description of the phase diagram obtained by solving (10) numerically, namely obtaining $T_C(p)$ as a function of p. They do however, severely restrict what can occur and so can be used as the basis of a classification scheme.

We are in a position to examine the phase diagrams of a system by solving (10) and (12) numerically. In order to compare them with the previous ones obtained for a disordered Ising binary alloy [2], the numerical results are shown for a square lattice ($z = 4$).

Figure 1 shows a classification of the phase diagrams of the system with $z = 4$ which is plotted in the space $(J_{AB}/\sqrt{J_A J_B}, J_B/J_A)$, for two selected values of r ($r = 1$ and $r = 0.7$).

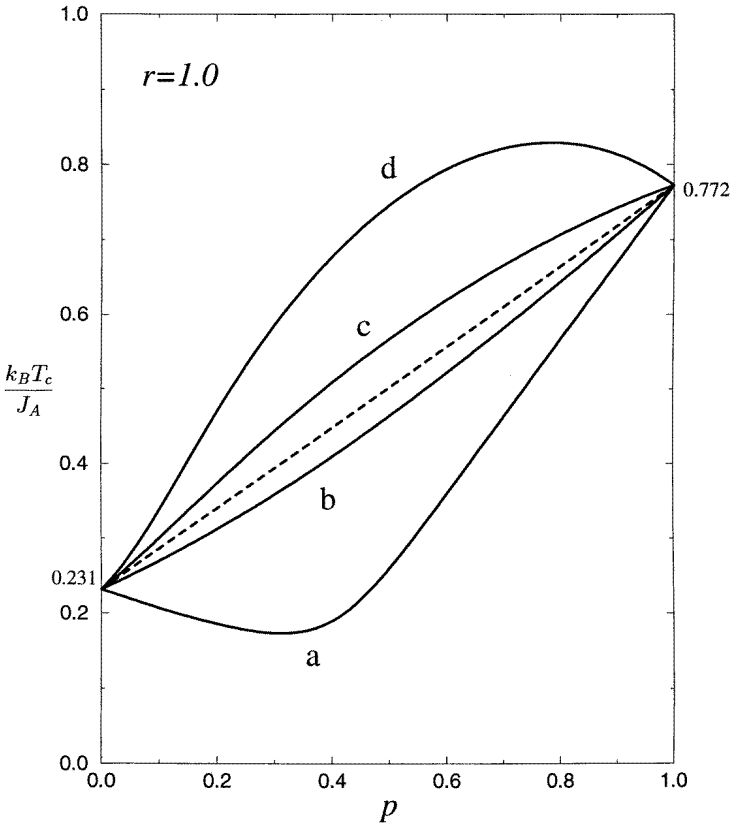

(a)

Figure 2. Complete phase boundaries for $z = 4$. The ratios $(J_{AB}/\sqrt{J_A J_B}, J_B/J_A)$ for the black points a–d marked in figure 1 are as follows: a: (0.2, 0.3); b: (1.0, 0.3); c: (1.5, 0.3) and d: (2.5, 0.3). The dashed lines are to guide the eye only. Parts (a) and (b) are respectively for $r = 1$ and $r = 0.7$.

The results have been determined from the initial slopes (12). In the figure, we used the same notation in describing the kinds of phase diagram as was used in [1–3], namely T, A, A′, B, B_1, S, S′, S_1 and S_1'. The results for $r = 1$ are equivalent to those found in [2] for the binary Ising alloy with $z = 4$. Only six kinds of phase diagram (A, A′, B, B_1, S and S′) are permitted from the nine possible phases. Comparing the results for $r = 1$ (solid lines) with those for $r = 0.7$ (dashed lines), the boundaries obtained from (12*a*) and (12*c*) are seen to be insensitive to the variation of r. In particular, with the decrease of r the region of parameter space in which S and S′ occur are extremely expanded, while the regions in which A and A′ occur become narrower in comparison with the corresponding regions for $r = 1$. Features similar to these have been also observed in the phase diagram of a binary alloy with random bonds [3]. Thus, such features may be specific characteristics resulting from the randomness in binary or ternary alloys.

In figure 2, the overall behaviour of $T_C(p)$ as a function of p is depicted; it was obtained by solving (10) numerically for the systems with $r = 1$ (figure 2(a)) and $r = 0.7$ (figure 2(b)), selecting the special values of J_{AB}, J_A and J_B that are labelled in figure 1 (the black points a–d in figure 1). At first sight, the diagrams seem very similar for the

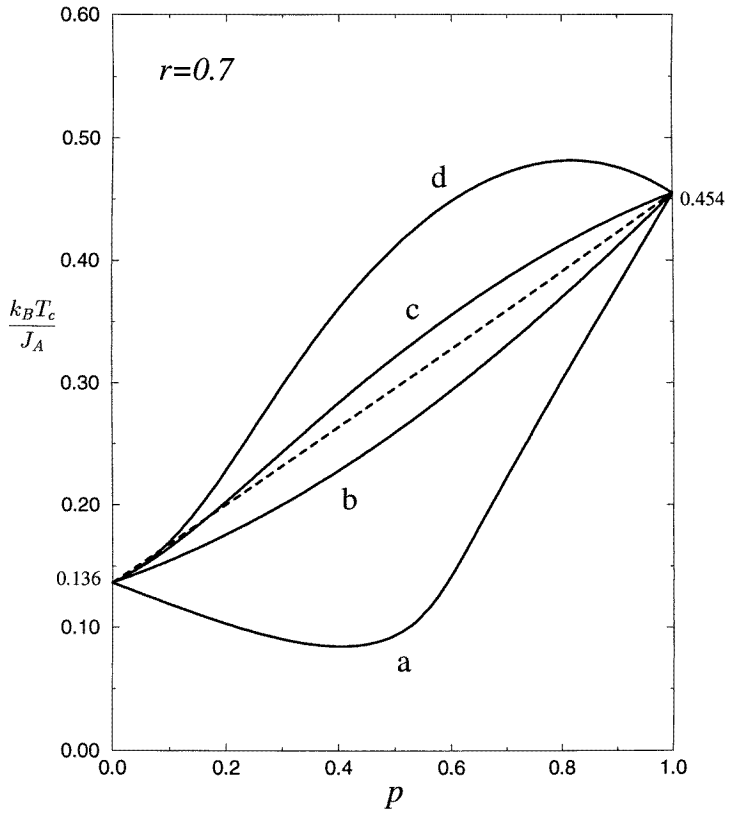

(b)

Figure 2. (Continued)

two ($r = 1$ or $r = 0.7$) cases. Looking at them in detail, however, one can find different behaviours of $T_C(p)$, especially in the vicinity of $p = 0$, as is expected from figure 1.

Finally, let us examine the effect of dilution on T_C for the ternary alloy by selecting the typical values of J_{AB}, J_A and J_B ($J_{AB}/J_A = 0.707$ and $J_B/J_A = 0.5$) labelled in figure 1 and changing the value of p. The results are shown in figure 3 for five values of p. In particular, the curves for $p = 1$ and $p = 0$ are equivalent to those for the dilution in the spin-$\frac{1}{2}$ Ising ferromagnet on a square lattice [14]. As discussed in [14], the critical concentration r_C at which $T_C(r)$ reduces to zero is given by $r_C = 0.4284$ for the systems with $p = 1$ and $p = 0$. When $0 < p < 1$, the T_C-curve as a function of r reduces to zero at the same critical concentration r_C as those for $p = 1$ and $p = 0$. This, indicates that the decoupling approximation (or the EFT) gives reasonable results for the present problem.

4. Ferrimagnetism in the system with $S_B = 3/2$

In this part, let us study the role of non-magnetic atoms in the magnetic properties of the disordered Ising ferrimagnetic ternary alloy with $z = 3$ and $S_B = \frac{3}{2}$, since in the previous work [4] the magnetic properties of the corresponding ferrimagnetic binary alloy A_pB_{1-p} have been examined.

The transition temperature T_C of a disordered ternary alloy is then determined from the

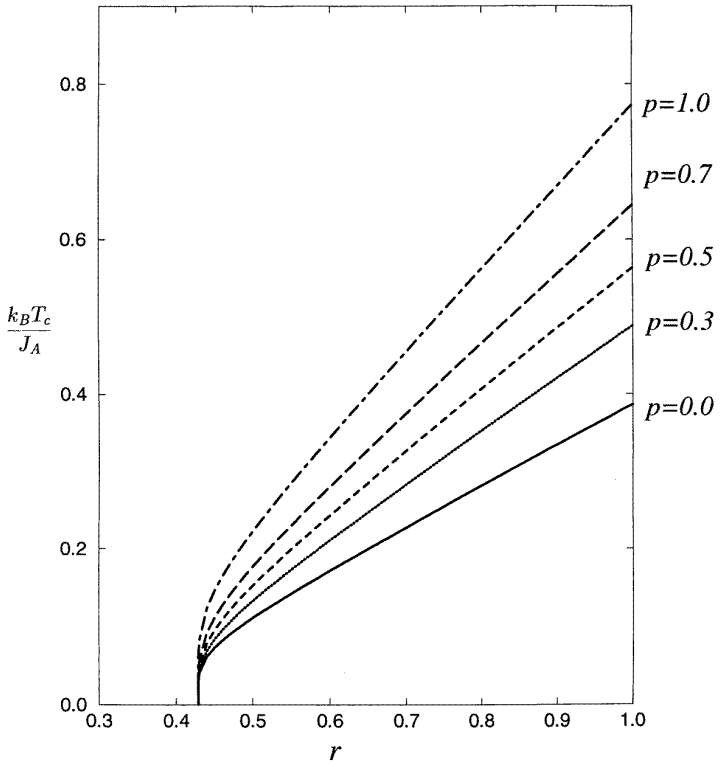

Figure 3. The concentration dependence of $T_{\mathrm{C}}(p)$ for the diluted Ising ternary alloy with $z = 4$, when the ratios $J_{\mathrm{AB}}/J_{\mathrm{A}}$ and $J_{\mathrm{B}}/J_{\mathrm{A}}$ are fixed at $J_{\mathrm{AB}}/J_{\mathrm{A}} = 0.707$ and $J_{\mathrm{B}}/J_{\mathrm{A}} = 0.5$ and various values of p are selected. The results for $p = 1$ and $p = 0$ are equivalent to those for the diluted Ising binary alloy with $z = 4$ [13].

relation

$$[2zrpK_1 - 1]\left[zr(1-p)\frac{R_2}{\eta_0} - 1\right] = 2(zr)2p(1-p)\frac{R_1 K_2}{\eta_0} \tag{13}$$

with

$$K_1 = \sinh\left(\frac{J_{\mathrm{A}}}{2}\nabla\right)\left[1 - r + r\left\{p\cosh\left(\frac{J_{\mathrm{A}}}{2}\nabla\right) + (1-p)\cosh(J_{\mathrm{AB}}\eta_0\nabla)\right\}\right]^{z-1} F_{\mathrm{A}}(x)\Big|_{x=0} \tag{14a}$$

$$K_2 = \sinh\left(\frac{J_{\mathrm{AB}}\eta_0}{2}\nabla\right)\left[1 - r + r\left\{p\cosh\left(\frac{J_{\mathrm{A}}}{2}\nabla\right) + (1-p)\cosh(J_{\mathrm{AB}}\eta_0\nabla)\right\}\right]^{z-1} F_{\mathrm{A}}(x)\Big|_{x=0} \tag{14b}$$

$$R_1 = \sinh\left(\frac{J_{\mathrm{AB}}}{2}\nabla\right)\left[1 - r + r\left\{p\cosh\left(\frac{J_{\mathrm{AB}}}{2}\nabla\right) + (1-p)\cosh(J_{\mathrm{B}}\eta_0\nabla)\right\}\right]^{z-1} F_{\mathrm{B}}(x)\Big|_{x=0} \tag{14c}$$

$$R_2 = \sinh\left(\frac{J_{\mathrm{B}}\eta_0}{2}\nabla\right)\left[1 - r + r\left\{p\cosh\left(\frac{J_{\mathrm{AB}}}{2}\nabla\right) + (1-p)\cosh(J_{\mathrm{B}}\eta_0\nabla)\right\}\right]^{z-1} F_{\mathrm{B}}(x)\Big|_{x=0} \tag{14d}$$

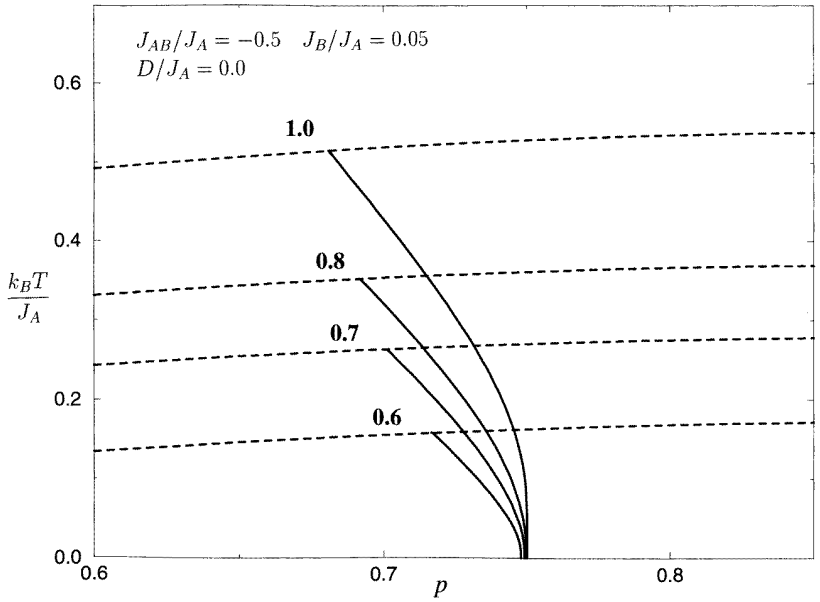

Figure 4. The phase diagram (T_C and T_{COMP} versus p curves) of the disordered ferrimagnetic ternary alloy with $z = 3$, when the parameters are fixed at $J_{AB}/J_A = -0.5$, $J_B/J_A = 0.05$, $D/J_A = 0.0$ and the value of r is changed from $r = 1.0$ to 0.6. The solid and dashed lines represent respectively the compensation temperature T_{COMP} and the Curie temperature T_C of the system.

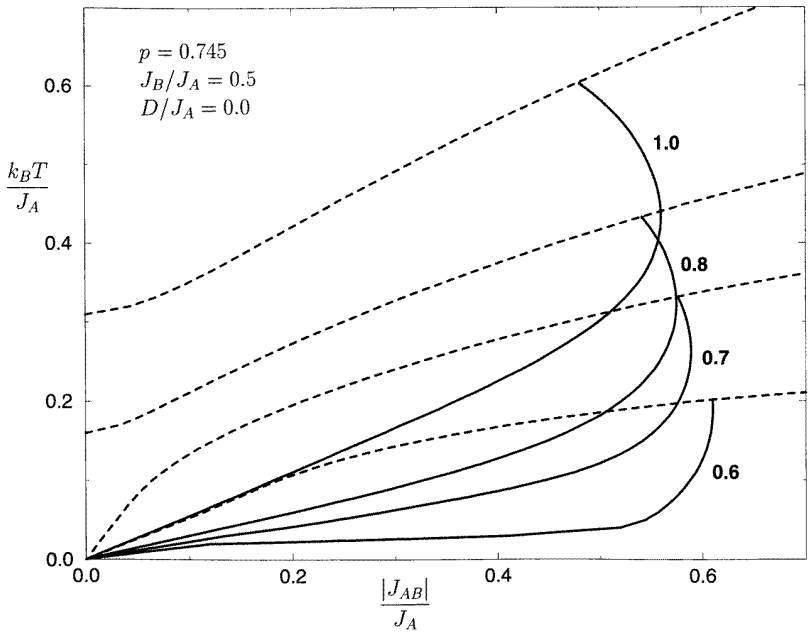

Figure 5. T_C (dashed line) and T_{COMP} (solid line) for the system with $z = 3$ plotted as a function of $|J_{AB}|/J_A$, when the parameters are fixed at $p = 0.745$, $J_B/J_A = 0.5$, $D/J_A = 0.0$, and the value of r is changed from $r = 1.0$ to 0.6.

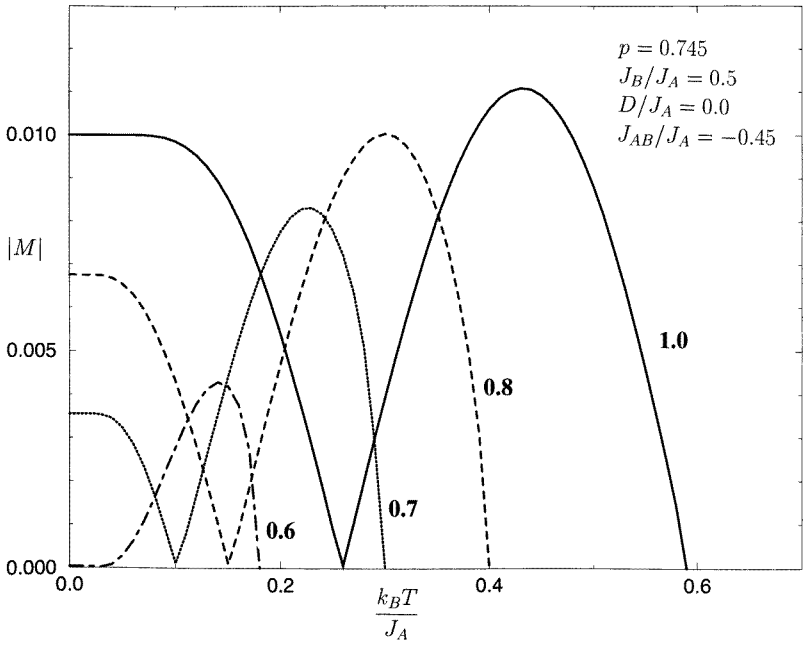

(a)

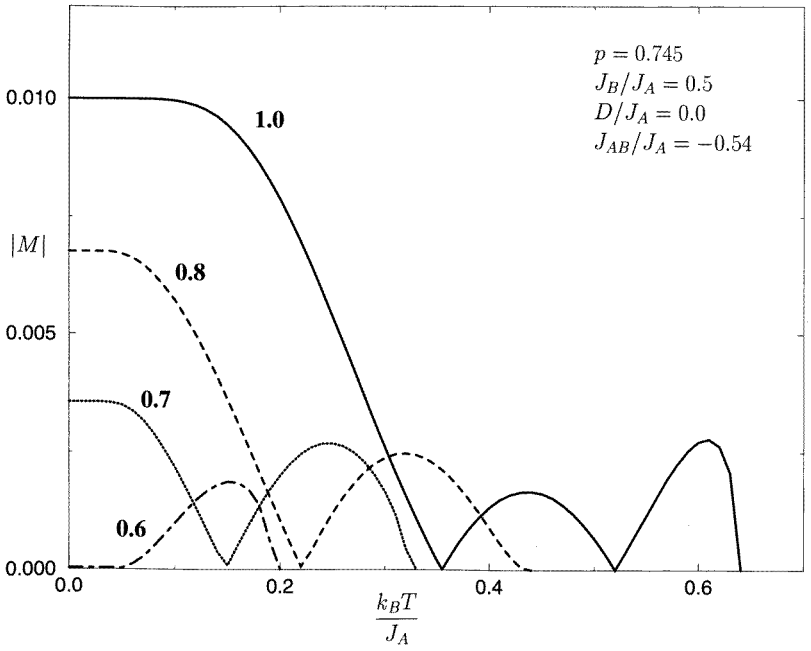

(b)

Figure 6. The $|M|/N$ versus T curves for the system with $p = 0.745$, $J_B/J_A = 0.5$, $D/J_A = 0.0$ and $z = 3$, when the value of r is changed from $r = 1.0$ to 0.6 and the three values of J_{AB}/J_A are selected from the phase diagram of figure 5; $J_{AB}/J_A = -0.45$ for panel (a), $J_{AB}/J_A = -0.54$ for panel (b), $J_{AB}/J_A = -0.59$ for panel (c).

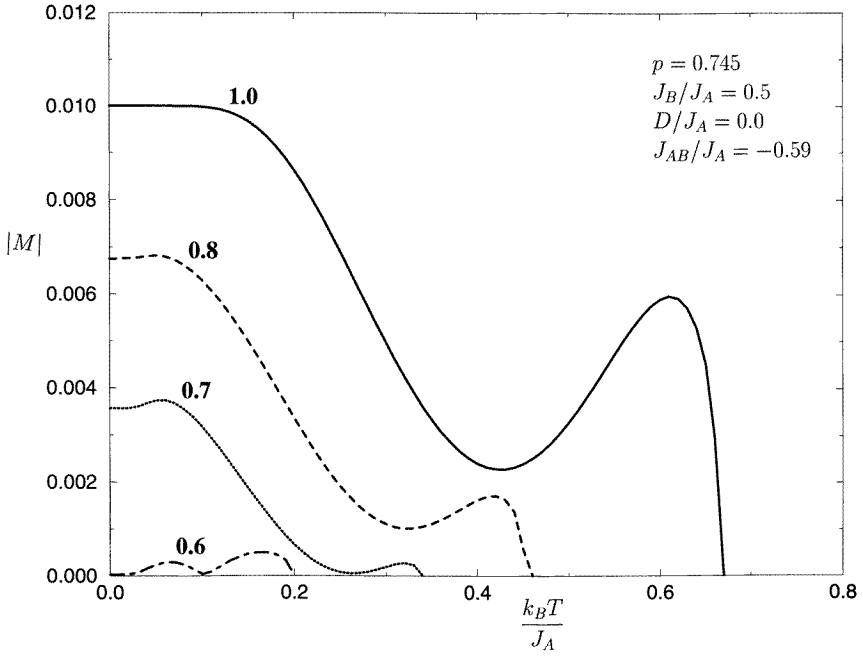

(c)

Figure 6. (Continued)

where the parameter η_0 can be evaluated from

$$(\eta_0)^2 = \left[1 - r + r\,p\cosh\left(\frac{J_{\mathrm{AB}}}{2}\right) + (1-p)\cosh(J_{\mathrm{B}}\eta_0\nabla)\right]^z G_{\mathrm{B}}(x)\Big|_{x=0}. \tag{15}$$

A compensation point, at which the total magnetization vanishes below the transition temperature, in the system can be determined by substituting the condition

$$\frac{M}{N} = 0 \tag{16}$$

in (2). Here, the following fact must be noted: the exchange interaction J_{AB} is given by a negative value, in order for the present system to be ferrimagnetic.

Let us now examine the magnetic properties of the ferrimagnetic system with $z = 3$ by solving (13), (9) and (16) numerically. Figure 4 shows a typical phase diagram (T_{C} and T_{COMP} versus p) for the ferrimagnetic system, when $J_{\mathrm{AB}}/J_{\mathrm{A}} = -0.5$, $J_{\mathrm{B}}/J_{\mathrm{A}} = 0.05$, $D/J_{\mathrm{A}} = 0.0$ and the value of r is changed. For real ferrimagnetic ternary alloys based on rare earths (RE) and transition metals (T), the relation $J_{\mathrm{A}}(J_{\mathrm{T-T}}) > -J_{\mathrm{AB}}(J_{\mathrm{RE-T}}) > J_{\mathrm{B}}(J_{\mathrm{RE-RE}})$ is normally satisfied. The solid and dashed lines represent the T_{COMP}- and T_{C}-curves, respectively. When $r = 1.0$, the T_{COMP}-curve reduces to zero at $p = 0.75$, since at $T = 0$ K, $S_{\mathrm{A}} = \frac{1}{2}$ and $S_{\mathrm{B}} = \frac{3}{2}$ in (16). With the decrease of r, the sublattice magnetizations at $T = 0$ K decrease from their saturation values, and hence the critical value of p at which $T_{\mathrm{COMP}} = 0$ may decrease a little, moving to the left-hand side, from $p = 0.75$. As shown in figure 4, the region of p in which a compensation point can be obtained becomes narrow, when the concentration of non-magnetic atoms increases. As far as we are aware, such a phenomenon has not previously been reported.

In [4], the possibility of more than one compensation point in a binary ferrimagnetic alloy with $z = 3$ has been discussed within the framework of the EFT, selecting $D/J_A = 0.0$, $J_B/J_A = 0.5$, $p = 0.745$ and changing the value of $|J_{AB}/J_A|$ (see figure 5(a) in [4]). Let us next study the effect of non-magnetic atoms on the T_{COMP}-curve for the ternary alloy system with $D/J_A = 0.0$, $J_B/J_A = 0.5$ and $p = 0.745$. The numerical results are depicted in figure 5. The solid and dashed lines denote the T_{COMP}- and T_C-curves, respectively. The results labelled $r = 1.0$ are equivalent to those in figure 5(a) of [4] and there is a possibility of two compensation points over a rather wide region of $|J_{AB}/J_A|$. The results of figure 5 indicate some interesting facts.

(i) The possibility of two compensation points becomes gradually less with the increase in the number of non-magnetic atoms.

(ii) The region of $|J_{AB}/J_A|$ in which one can find a compensation point becomes wider with the decrease of r from $r = 1$.

In particular, phenomenon (ii) is clearly different to what is shown in figure 4.

In order to clarify the prediction of figure 5, the temperature dependence of the total magnetization $|M|/N$ in the system with $p = 0.745$, $J_B/J_A = 0.5$ and $D/J_A = 0.0$ has been plotted in figure 6, selecting the special values of J_{AB}/J_A chosen in figure 5: -0.45 for figure 6(a), -0.54 for figure 6(b) and -0.59 for figure 6(c). As is seen from the figures, one can find some characteristic magnetization curves not predicted in the Néel theory of ferrimagnetism [15, 16], such as the curve labelled $r = 0.7$ in figure 6(c).

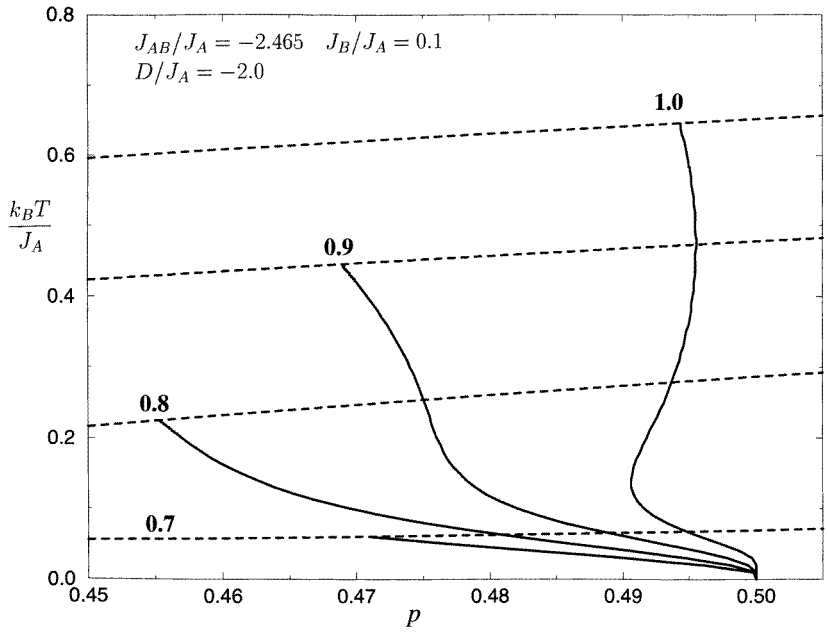

Figure 7. The phase diagram of the ferrimagnetic system obtained with $z = 3$, $J_{AB}/J_A = -2.465$, $J_B/J_A = 0.1$, $D/J_A = -2.0$ and with the concentration near $p = 0.5$, when the value of r is changed from $r = 1.0$ to 0.7. The solid and dashed lines represent respectively the compensation temperature T_{COMP} and the Curie temperature T_C of the system.

Figure 7 shows the possibility of three compensation points in the system with $J_B/J_A = 0.1$, $J_{AB}/J_A = -2.465$, $D/J_A = -2.0$ and $r = 1.0$; the result is consistent

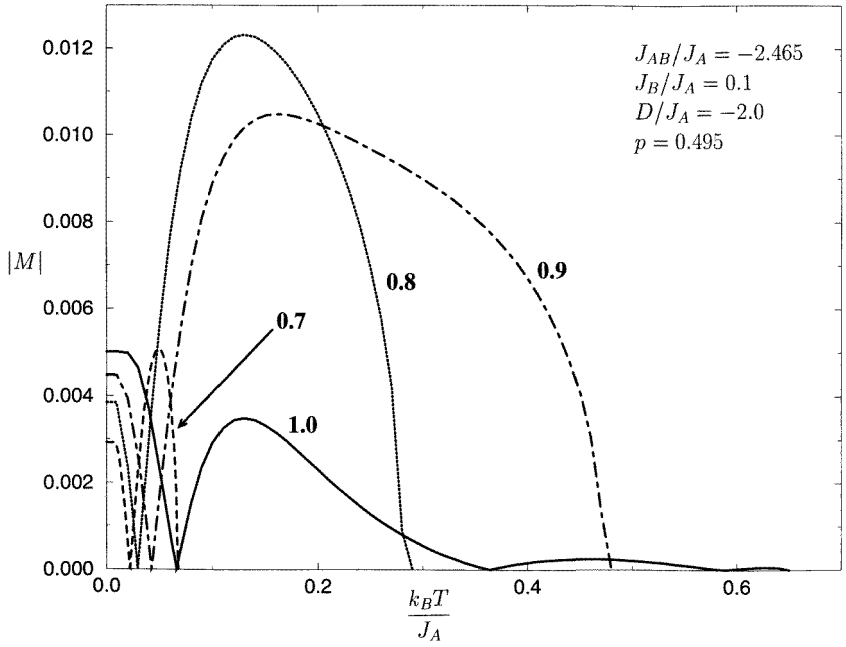

Figure 8. The $|M|/N$ versus T curves for the system obtained with $p = 0.495$, $J_{\rm AB}/J_{\rm A} = -2.465$, $J_{\rm B}/J_{\rm A} = 0.1$, $D/J_{\rm A} = -2.0$ and $z = 3$, when the value of r is changed from $r = 1.0$ to 0.7.

with that of figure 6(a) in [4]. With the decrease of r, the possibility immediately becomes an impossibility. For the systems with $r = 0.9$ and 0.8, only one compensation point is observed over a wide range of p, although the region in which one can find a compensation point for the system with $r = 0.7$ becomes narrower than that for $r = 0.8$. In particular, the effect of non-magnetic atoms on the temperature dependence of M/N for the system with $p = 0.495$, $J_{\rm B}/J_{\rm A} = 0.1$, $J_{\rm AB}/J_{\rm A} = -2.465$ and $D/J_{\rm A} = -2.0$ is shown in figure 8, for four selected values of r. The figure also shows that the three compensation points for the system with $r = 1$ quickly become impossible with the decrease of r.

5. Conclusions

In this work, we have discussed the theoretical framework for the magnetic properties of a disordered Ising ternary alloy $(A_pB_{1-p})_rC_{1-r}$ consisting of two kinds of magnetic atom, A and B, with spins $S_{\rm A} = \frac{1}{2}$ and $S_{\rm B} = S$ $(>\frac{1}{2})$, and a non-magnetic atom C, on the basis of the effective-field theory with correlations. The formulation given in section 2 can be applied to any system with a certain value of S.

In section 3, the formulation was applied to the examination of phase diagrams for the system with $z = 4$ (the square lattice) and $S_{\rm A} = S_{\rm B} = \frac{1}{2}$. As depicted in figures 2 and 3, the numerical results are reasonable, which also implies that the decoupling approximation (8) (or the EFT) has physical meaning. Figure 1 clearly shows that with dilution the regions representing the phases A and A′ decrease and instead the regions representing S and S′ may increase, although the number of possible phases is always fixed at six. We have compared our model system without non-magnetic atoms to real materials such as

Fe–Co-based amorphous alloys and found good agreement [17].

In section 4, we have examined the effects of non-magnetic atoms on the magnetic properties of the disordered ferrimagnetic Ising ternary alloy with $z = 3$. With the decrease of r, as shown in figure 4, the T_{COMP}-curve for a system with $J_{\mathrm{A}} > -J_{\mathrm{AB}} > J_{\mathrm{B}}$ becomes narrow in the region of $|J_{\mathrm{AB}}/J_{\mathrm{A}}|$. As shown in figures 5 and 7, the possibility of more than one compensation point in the ferrimagnetic binary alloy with $r = 1$ is easily removed by substituting non-magnetic atoms into the alloy. Some interesting thermal variations of the total magnetization in the ferrimagnetic system are expected with the decrease of r, as depicted in figure 6(c).

Finally, the present formulation discussed in section 2 can be applied to a disordered Ising ternary alloy with an arbitrary value of S_{B}, while in this work we have discussed only the two systems with $S_{\mathrm{B}} = \frac{1}{2}$ and $S_{\mathrm{B}} = \frac{3}{2}$. We assume that study of a ferrimagnetic ternary alloy system with $S_{\mathrm{B}} =$ an integer spin value will be interesting, since tricritical behaviour may be found for this system with a negative value of D [18]. We hope to investigate this problem in the future.

References

[1] Thorpe M F and McGurn A R 1979 *Phys. Rev.* B **20** 2142
[2] Honmura R, Khater A F, Fittipaldi I P and Kaneyoshi T 1982 *Solid State Commun.* **41** 385
[3] Kaneyoshi T and Li Z Y 1987 *Phys. Rev.* B **35** 1869
[4] Kaneyoshi T and Jascur M 1993 *J. Phys.: Condens. Matter* **5** 3253
[5] Kaneyoshi T 1995 *J. Magn. Magn. Mater.* **140–144** 261
Kaneyoshi T 1995 *Physica* B **210** 178
[6] Kaneyoshi T 1994 *J. Phys.: Condens. Matter* **6** 1069
Jascur M and Kaneyoshi T 1997 *Phys. Status Solidi* b **203** 507
[7] Kaneyoshi T 1992 *Introduction to Amorphous Magnets* (Singapore: World Scientific)
[8] Moorjani K and Coey J M D 1984 *Magnetic Glasses* (Amsterdam: Elsevier)
[9] Luborsky F E 1980 *J. Appl. Phys.* **51** 2808
[10] Honmura R and Kaneyoshi T 1979 *J. Phys. C: Solid State Phys.* **12** 3979
[11] Kaneyoshi T, Tucker J W and Jascur M 1992 *Physica* A **186** 495
[12] Kaneyoshi T 1993 *Acta Phys. Pol.* A **83** 703
[13] Zernike F 1940 *Physica* **7** 565
[14] Kaneyoshi T, Tamura I and Sarmento E F 1983 *Phys. Rev.* B **28** 6491
[15] Néel L 1948 *Ann. Phys., Paris* **3** 137
[16] Herpin A 1968 *Theorie du Magnetisme* (Saclay: Presses Universitaires de France)
[17] Kaneyoshi T 1986 *Phys. Rev.* B **34** 7866
[18] Kaneyoshi T 1984 *Amorphous Magnetism* (Boca Raton, FL: Chemical Rubber Company Press)